

Controlled release of paraquat from surface-modified zeolite Y

Haoyu Zhang, Yanghee Kim, Prabir K. Dutta *

Department of Chemistry, 120 West 18th Avenue, The Ohio State University, Columbus, OH 43210, USA

Received 1 August 2005; received in revised form 29 September 2005; accepted 30 September 2005

Available online 16 November 2005

Abstract

The surface hydroxyl groups of zeolite Y were reacted with 1,1,3,3-tetramethyldisilazane, $\text{HN}(\text{SiHMe}_2)_2$ under ambient conditions and the grafting of siloxy functionality on the zeolite was confirmed by infrared, NMR spectroscopy and elemental analysis. Paraquat (methyl viologen) was ion-exchanged into the zeolite, followed by treatment with the disilazane reagent. Surface modification of paraquat-loaded zeolites encapsulates the guest molecules in the zeolite cages and release of paraquat by ion-exchange with sodium ions was studied. The total amount of paraquat released was dependent on the concentration of Na^+ in solution, and was similar for the derivatized and underivatized samples. In the absence of surface modification, equilibration occurred within 20 min, whereas with surface modification, the equilibration time was extended to 7 days. These kinetics are reflected in the effective diffusion coefficients (D) of paraquat, with $D = 1.2 \times 10^{-15} \text{ cm}^2 \text{ s}^{-1}$ for derivatized zeolite Y and $D = 0.2\text{--}1.1 \times 10^{-7} \text{ cm}^2 \text{ s}^{-1}$ for the underivatized sample. Paraquat was chosen as the guest molecule, since it is widely used as an herbicide and its controlled release is of interest in agricultural applications. © 2005 Elsevier Inc. All rights reserved.

Keywords: Methyl viologen; Pore narrowing; Drug release; Dosage control

1. Introduction

Controlled release has been employed extensively in food, agriculture, and pharmaceutical industries to deliver active substances such as drugs, pesticides, herbicides and fertilizers [1]. A diverse group of materials have been investigated as controlled release systems, such as naturally occurring polymeric materials [2], synthetic hyperbranched dendrimers [3] and organic hollow microspheres [4]. Polymers are the most commonly used materials for controlled release [5]. The active agent is usually dispersed in the polymeric matrix by means of compression, dissolution or melting, and agent release is dependent on the polymer and the loading level of the agent. Uneven distribution of active agents in the matrix is considered a limitation in optimum controlled release [6]. Therefore, porous materi-

als with well-ordered structures are attractive candidates for storage and release of organic guest molecules.

Zeolites have a well-defined nanopore structure with a crystalline framework consisting of SiO_4 and AlO_4 tetrahedra. The presence of Al in the zeolite framework leads to a charged framework and cation-exchange capabilities [7]. Ion-exchange can be used to load agents as well as release them, and the high ion-exchange capacity improves the loading of agents. Because of these properties, zeolites have been used to control release of fertilizer components [8], as a carrier for pesticides [9] and for demonstration of drug delivery using model systems [10,11]. In addition to zeolites (pore diameters $< 10 \text{ \AA}$), mesoporous materials (pore diameters $\approx 20\text{--}500 \text{ \AA}$) such as MCM-41 have also been examined for controlled release [12–15]. Site-specific delivery has also been reported by grafting receptor functional groups on surface of mesoporous materials [16].

The passage of guest molecules through zeolite pores can be controlled by pore size engineering [17]. Due to the presence of silanol groups on zeolite surfaces, silylation is one of most commonly used methods for surface

* Corresponding author. Tel.: +1 614 292 4532; fax: +1 614 688 5402.

E-mail addresses: dutta.1@osu.edu, dutta@chemistry.ohio-state.edu (P.K. Dutta).

modification [18]. Zeolites with narrowed pore sizes will also influence loading of agents. To achieve optimum storage with slow release, pore modification of the zeolite needs to occur after loading. However, most modification methods require harsh conditions, such as high temperature, and presence of strong acids or bases [19]. In these cases, the encapsulated agents can be destroyed or lose their activities. Therefore, surface modification under mild condition is necessary. Recently, Anwender et al. presented a surface modification strategy of MCM-41 via silazane silylation, which can take place under mild conditions [20]. We have adapted this method to zeolites for the first time and demonstrate the efficacy of the pore narrowing for controlled release of paraquat.

Zeolite Y, chosen as the host system has a three-dimensional structure with 7.4 Å diameter window openings connecting 13 Å diameter supercages [7]. Paraquat which has a dimension of $13.4 \times 6.4 \times 3.4$ Å [21] can be readily ion-exchanged into the zeolite [22]. Paraquat is one of most commonly used herbicides and is also referred to as methyl viologen. Its characteristic electronic spectrum can be used to estimate the release from zeolites into solution. In the present study, a paraquat loaded zeolite Y was modified under ambient conditions by using $\text{HN}(\text{SiHMe})_2$ (TMDS) as silylating reagent. The resulting material was characterized by infrared, NMR spectroscopy, and elemental analysis. The amounts of paraquat as well as release kinetics of paraquat from modified zeolites via ion-exchange with Na^+ in solution were studied.

2. Experimental

2.1. Chemicals

Sodium zeolite Y (Union Carbide LZY-52) was calcined at 500 °C in air to remove organic impurities. 1,1,3,3-tetramethyldisilazane (TMDS), paraquat (methyl viologen dichloride hydrate, MVCl_2) were purchased from Aldrich chemicals and used as received. *n*-Hexane was dried prior to use.

2.2. Paraquat loading

The loading of paraquat was achieved by ion-exchange. In a typical experiment, 1.0 g zeolite Y was mixed with 95 mg paraquat, 10 ml deionized water was added and the mixture was stirred for 24 h at room temperature. Then, the paraquat-loaded zeolite was washed thoroughly with deionized water and dried at 40 °C. To reach maximum loading level, the loading experiment was repeated twice.

2.3. Silylation experiments

The silylation procedure was similar to that reported in the literature [20]. One hundred milligram paraquat-loaded zeolite Y was dehydrated under high vacuum ($>10^{-4}$ Torr)

at ambient temperature for 3 days. The dehydrated sample was then transferred to a nitrogen-filled glovebox, and 30 ml dried *n*-hexane was added. The mixture was sonicated for 1 h to break the zeolite aggregates and improve dispersion. To this suspension, 20 µl TMDS was added and the mixture was stirred at room temperature for 1 h. The particles were filtered and washed thoroughly with dried *n*-hexane. The silylated zeolite was dried under vacuum at room temperature.

2.4. Release of paraquat

Release of paraquat from the zeolite was done by ion-exchange with NaCl solutions of 1.0 M, 0.1 M, and 0.01 M concentrations. Typically, 20 mg silylated material was well-suspended in a 100 ml NaCl solution, and the mixture was stirred at room temperature. The concentration of paraquat released into the solution at predetermined time intervals was determined by taking the supernatant fluid and measuring its absorbance ($\lambda_{\text{max}} = 257$ nm, $\epsilon = 20,700 \text{ M}^{-1} \text{ cm}^{-1}$ [23]) on a spectrophotometer (Shimadzu UV-265). After each measurement, the fluid was returned to the original mixture. The fraction of release versus time was calculated. The experiment was repeated three times and the average is reported.

2.5. Characterization

2.5.1. Elemental analysis

C, H, N analysis of the silylated samples were carried out by the Galbraith laboratories, Tennessee.

2.5.2. Diffusion-reflectance infrared Fourier transform (DRIFT) spectroscopy

DRIFT measurements were made using a Bruker Instruments (Billerica, MA) IFS-66s Fourier Transform Infrared Spectrometer equipped with a globar source, KBr beamsplitter and a DTGS detector. The variable aperture was at its maximum setting (12 mm), and spectra were obtained at 6 cm^{-1} resolution. In most cases, 1000 scans were averaged and were processed with a Blackman-Harris three-term apodization function and Mertz phase correction. Sampling was performed using a Spectra-Tech (Shelton, CT) Collector/Environmental Chamber.

2.5.3. MAS NMR spectroscopy

All samples were heated at 250 °C under high vacuum (10^{-4} Torr) for 3 h. Approximately 100 mg of sample was placed inside a 4 mm (outside diameter) rotor with Kel-F cap (3 M, Minneapolis, MN). Single pulse excitation was applied (pulse repetition 5 s, $\pi/2$ pulse, spinning speed 13 kHz). The ^{13}C MAS NMR spectra were recorded at 75.483 MHz by application of a ramped-amplitude cross-polarization (CP) pulse sequence (pulse repetition 2 s, $\pi/2$ ^1H excitation pulse, 2000 µs ^{13}C contact pulse, spinning speed 13 kHz) and composite pulse TPPM decoupling. The spin-locked carbon pulse power in the CPMAS

sequence was ramped linearly from one half its maximum values as described by Metz et al. [24]. The Hartman–Hahn matching conditions and TPPM parameters were optimized using polycrystalline glycine. Background ^{13}C CPMAS spectra were acquired under identical conditions and subtracted from sample spectra. All of the spectra were referenced to $\text{Si}(\text{CH}_3)_4$.

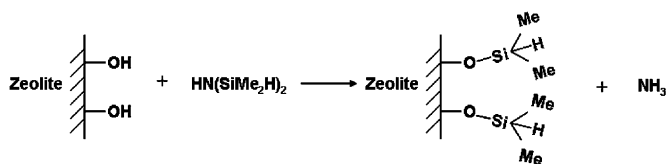
2.5.4. Scanning electron microscopy (SEM)

Scanning electron micrographs were recorded on gold coated TMDS-modified zeolite Y samples on a Phillips XL-30 ESEM, operating at 30 kV accelerating current.

3. Results

3.1. Silylation and characterization

The reaction of surface hydroxyl groups of zeolite Y with TMDS is expected to proceed as shown below [20]:



Several spectroscopic studies were carried out to monitor the derivatization process. Diffuse reflectance infrared spectroscopy (DRIFT) of unmodified and modified zeolite Y is shown in Fig. 1. A sharp band at 3700 cm^{-1} indicative of isolated or terminal silanol groups in underivatized zeolite [18,25] is absent after treatment with TMDS. In addition, the asymmetric and symmetric stretching bands due to CH_3 group of TMDS are observed at 2966 cm^{-1} and 2903 cm^{-1} , respectively. The broad band at 3400 cm^{-1} is assigned to intrazeolitic water. Complete dehydration of

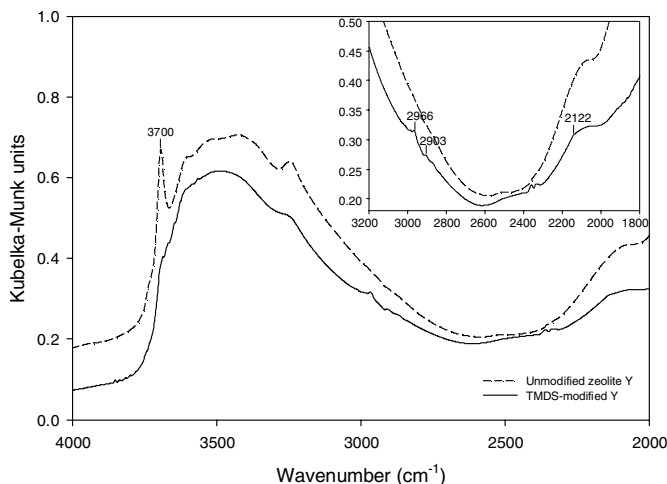


Fig. 1. Infrared (DRIFT) spectra of the unmodified and TMDS-modified zeolite Y.

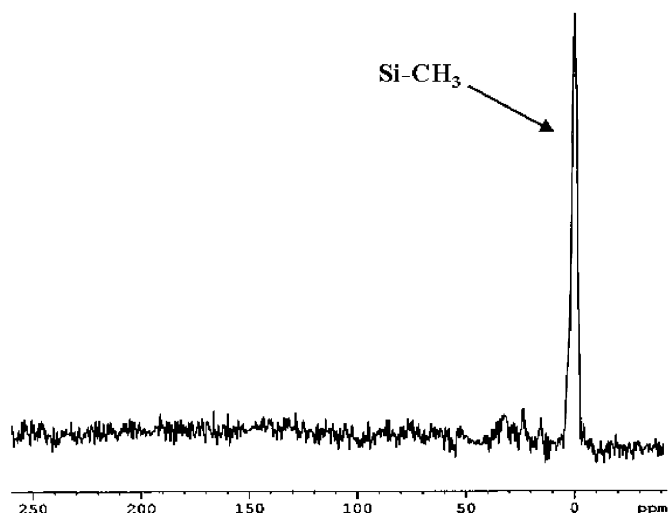


Fig. 2. ^{13}C MAS NMR spectrum of the TMDS-modified zeolite Y.

the zeolite would require temperatures in excess of $500\text{ }^\circ\text{C}$ and would destroy the paraquat, so dehydration was done under vacuum at ambient temperatures. A weak, broad band at 2122 cm^{-1} due to Si–H stretch is also observed [20]. The disappearance of the terminal silanol groups indicate that they are the active sites for grafting [20,26]. Fig. 2 shows the ^{13}C MAS NMR spectrum of TMDS-modified Y and the peak at 0 ppm is assigned to the Si– CH_3 [20].

Fig. 3 shows the electron micrographs of the derivatized zeolite sample, indicating dispersed zeolite particles with an average size of $0.6\text{ }\mu\text{m}$.

The surface coverage of TMDS groups was calculated based upon the carbon content of the derivatized zeolites. The % of C in the TMDS-modified zeolite Y was determined by elemental analysis to be 0.65%. Assuming that the morphology of zeolite particles is spherical with an average diameter of $0.6\text{ }\mu\text{m}$ and the density of zeolite to be 1.25 g cm^{-3} , surface coverage is calculated to be $34\text{ }\mu\text{mol m}^{-2}$ (0.27 mmol g^{-1} of zeolite). This loading level is higher than the number of silanol groups on zeolites (0.056 mmol g^{-1} [27]) by a factor of 5. Our hypothesis is that the TMDS is forming a polymer on the zeolite surface; the Si–H bond can be activated by acid catalysts and prone to attack by water [28]. The aluminum sites on the zeolite can act as weak Lewis acids, and the water in the zeolite can help in the polymerization process. The polymerization would lead to loss of Si–H bonds (except for the terminal ones) and would also explain the weakness of the 2122 cm^{-1} band.

3.2. Release of paraquat

Release of paraquat from underivatized and derivatized zeolites Y was examined by suspending a fixed amount of the zeolite into 1.0, 0.1, and 0.01 M NaCl solutions. The amount of paraquat released into the aqueous phase as a function of the time was monitored by the characteristic band of paraquat at 257 nm . Fig. 4 compares the release

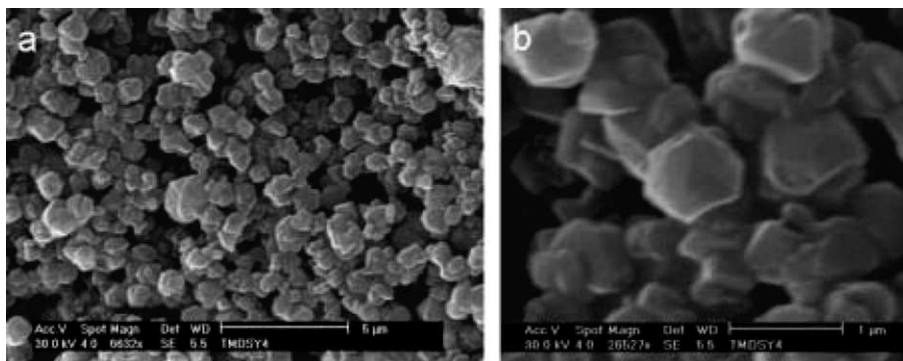


Fig. 3. Scanning electron micrographs of the TMDS-modified zeolite Y.

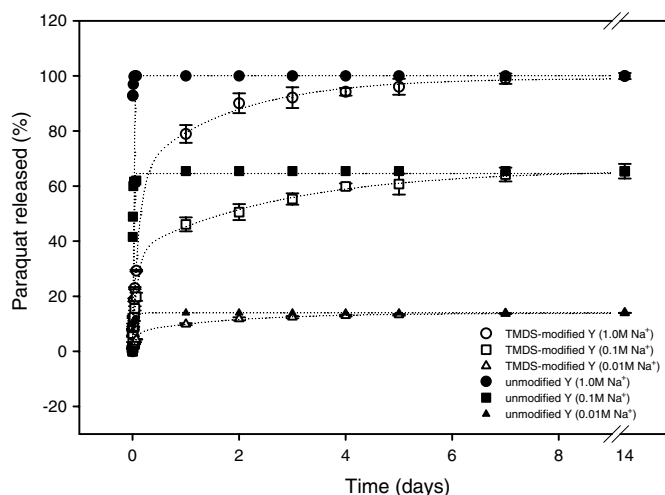


Fig. 4. Release of paraquat from unmodified and TMDS modified zeolite Y as a function of time in 1.0 M, 0.1 M, and 0.01 M NaCl.

of paraquat versus time for unmodified and modified zeolites. Similar equilibrium values, controlled by the $[\text{Na}^+]$ in solution were reached for both unmodified and modified samples. At the $[\text{Na}^+] = 1.0 \text{ M}$, all of the paraquat is expected to be released from the zeolite [22], whereas for $[\text{Na}^+] = 0.1$ and 0.01 M , the total release was 65% and 14% of the total paraquat in the zeolite. These results are consistent with the fact that extent of ion-exchange is determined by the ionic strength of solutions. The major change upon TMDS-modification is that the rate of release is considerably reduced. For all unmodified zeolites, the equilibrium is reached within 20 min, as shown in Fig. 5 for the first 100 min of the ion-exchange reaction. In contrast, the time to reach equilibrium for the modified zeolites was greater than 7 days in all three cases. Thus, the extent of ion-exchange is controlled by the ionic strength of the solution, and surface modification determines the rate of paraquat release.

4. Discussion

In this paper, we have presented a new strategy to modify the pore structure of zeolites loaded with fragile organic

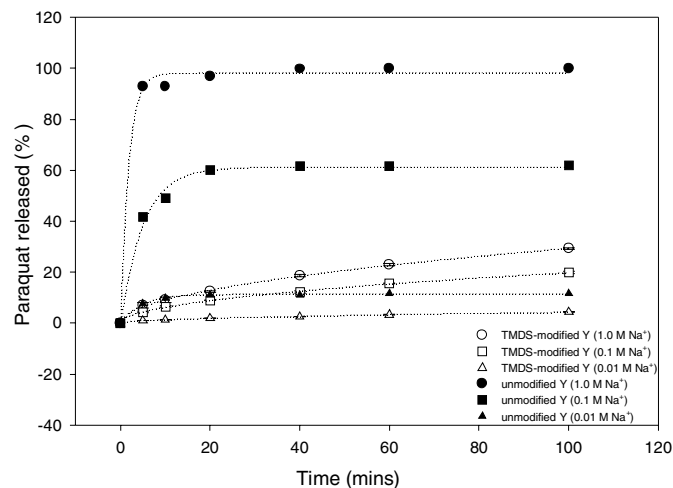
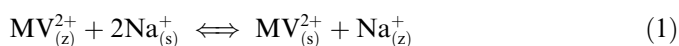


Fig. 5. Release of paraquat from unmodified and TMDS modified zeolite Y during the first 100 min in 1.0 M, 0.1 M, and 0.01 M NaCl.

molecules. Spectroscopic studies indicate that even under mild reaction conditions and short reaction times, TMDS groups were successfully grafted on the surface of zeolites. Because of the mild conditions, there was no damage to the intrazeolitic paraquat molecules, as evidenced by the fact that the total amount released after modification was comparable to the unmodified sample. The advantage of surface modifications post-loading is that the maximum loading level can be maintained. The loading of paraquat, determined by ion-exchange with 1.0 M Na^+ was estimated to be 0.75 mmol g^{-1} of zeolite (14% by weight). All of the Na^+ ions in the zeolite are not replaced by paraquat because its size limits its entry into only the large supercages and not the sodalite cages. Comparable numbers in the literature for complete loading levels of paraquat in zeolite Y range from 0.85 to 1 mmol g^{-1} of zeolite, but since the level of hydration of the zeolite as well as the Si/Al ratio varies between different studies, the absolute loading levels cannot be directly compared [22,29]. At maximum paraquat loading (in the present study ~ 1.5 molecules per supercage), about 90% of the possible supercage occupancy is taken up and paraquat is expected to be homogeneously distributed in the zeolite particles [22].

The release of paraquat (MV^{2+}) from zeolites can occur only via ion-exchange since charge neutrality of the zeolite framework needs to be maintained. The ion-exchange process is represented by the following equation:



where subscripts denote zeolite or solution phase. The equilibria of exchange of small monovalent and divalent cations have been investigated for a variety of zeolites [30]. Equilibrium constant for exchange of paraquat and sodium ion in zeolite Y has also been measured [22], and depends on the activity of the exchanging ions. At the higher Na^+ concentration (1.0 M), the equilibrium represented by (1) lies farther to the right, and the total release amount approaches the capacity of zeolites. At the lower Na^+ concentrations (0.1 M, 0.01 M), the total release amount was decreased to 65% and 14%, respectively. Most importantly, for similar Na^+ concentrations, there is no significant difference of amounts released between modified and unmodified samples, indicating that surface modification has no effect on the equilibrium of ion-exchange. These results also demonstrate that the total amount of paraquat release can be controlled e.g. above an effective level but below a toxic level, by using different concentrations of the ion-exchanging cation.

Kinetics of ion-exchange process in zeolites has been extensively studied and two processes, diffusion within the zeolite (particle diffusion) and diffusional transport through the liquid film surrounding the particle (film diffusion) are proposed as important steps in the ion-exchange process [31,32]. In the TMDS-modified zeolite, the particle diffusion model has two parts: intrazeolitic diffusion of ions within the zeolite framework, as well as out of the zeolite through the TMDS modified surface, with the rate controlling step being determined by the slower of the two steps. The particle diffusion model predicts that the fractional exchange (F) should be independent of Na^+ concentrations and at short times can be given by [32]:

$$F = \frac{Q_t}{Q_\infty} = \frac{6}{r} \sqrt{\frac{Dt}{\pi}} \quad (2)$$

where Q_t and Q_∞ are the amounts of exchange at time t and equilibrium (∞), respectively. D represents the effective diffusion coefficient of the exchanging ions (paraquat) in zeolite particles, and r is the mean radius of the zeolite particles. Fig. 6 shows the plots of F versus time for the three concentrations of Na^+ examined in this study. The rates of release of paraquat from the zeolite are similar for all three concentrations, with some variation around the 2-day observation point. In addition, the insert of Fig. 6 shows that the linear relationship between F and \sqrt{t} as predicted by the particle diffusion model indeed holds true for short times ($t \leq 100$ min). The effective diffusion coefficient, D , obtained from the slope of the F versus \sqrt{t} plot is calculated to be $1.2 \times 10^{-15} \text{ cm}^2 \text{ s}^{-1}$. The values of D of paraquat in underivatized zeolite Y ranges from $1.1 \times 10^{-7} \text{ cm}^2 \text{ s}^{-1}$ [33] to $2 \times 10^{-8} \text{ cm}^2 \text{ s}^{-1}$ [22]. Intrazeolitic diffusion of paraquat

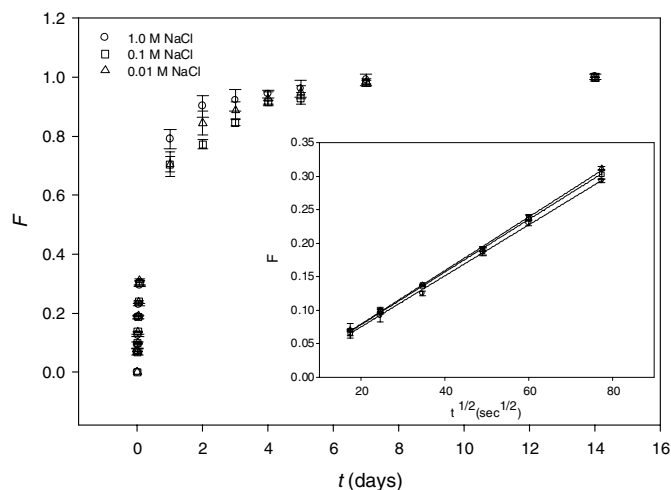


Fig. 6. The fraction of release of paraquat (F) versus t plots: the slope of the initial portion of the F versus $t^{1/2}$ curve is obtained to be $4 \times 10^{-3} \text{ s}^{-1/2}$ (see inset for plot of F versus $t^{1/2}$).

occurs through the 12-ring, 7.4 \AA apertures between the supercages and equilibrium is achieved rapidly within 20 min for the 0.01 M Na^+ and considerably faster for the 1.0 M Na^+ solution. In literature, the time to establish equilibrium for high ionic strength solutions is reported to be of the order of seconds [22]. In contrast, the release rate was significantly reduced for TMDS-modified zeolite Y, only due to the decrease in rate of paraquat diffusion through the blocked windows at the zeolite-solution interface, since the interior of the zeolite is not modified. Fig. 7 shows a schematic representation of the surface modification. The $Si(Me)_2$ -groups on the zeolite pores have enough mobility to allow for the entry and release of the Na^+ and paraquat ions, but their presence does provide a barrier to motion from zeolite into solution.

Even though this study is one of the first examples of a surface-modified zeolite for release of organic molecules, the use of coated ion-exchange resins for controlled release of ions has been well-studied and serves as a useful comparison [34–37]. The nature of the coating in these resin studies is typically a semipermeable membrane and the release of molecules is retarded due to diffusion through the membrane. Interestingly, the mechanism of the coated and uncoated resins tends to follow the particle diffusion model of ion-exchange [35]. Problems with polymer membrane coatings include the presence of microcracks that lead to rapid release of molecules [36]. Another strategy has been to reduce the diffusion rate within the particle by gelation of a polymeric material [37].

In comparison to ion-exchange resins, the zeolite system provides several advantages. First, the slower release rate is primarily controlled by molecular sieving rather than diffusion through a barrier. Second, there are a large number of disilazanes of different structures that are available for surface derivatization, providing the ability to tune the window size of the zeolite and thereby alter release rates [20].

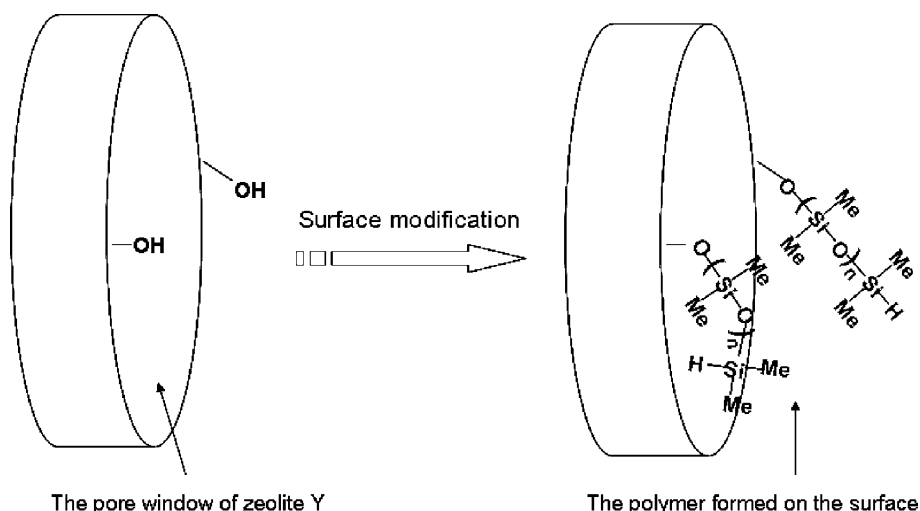


Fig. 7. Schematic representation of the surface modification of zeolite Y by TMDS.

5. Conclusion

We have demonstrated the feasibility of storage and controlled release of paraquat from surface-modified zeolite Y. Paraquat was trapped within the zeolite pores by ion-exchange followed by surface modification under mild conditions by reaction with 1,1,3,3-tetramethyldisilazane. The release of paraquat into aqueous solution by ion-exchange with sodium ions was studied. The total release amount was dependent on the concentration of sodium ions in solution, and the release rate on the surface modification. After surface derivatization, the release was decreased to a period of one week as compared to 20 min for underivatized zeolites, which suggests that the present derivatization process has the potential to make zeolites an effective material for slow-release of reagents. A particle diffusion model of ion-exchange was found to satisfactorily explain the data for the modified zeolites.

Acknowledgments

We acknowledge funding by NASA and thank Mr. William Hockaday for help with the solid-state NMR measurements.

References

- [1] R. Duncan, L.W. Seymour, *Controlled Release Technologies: A Survey of Research and Commercial Applications*, Elsevier Advanced Technology, Oxford, 1989.
- [2] S. Bogdanský, *Drugs Pharm. Sci.* 45 (1990) 231–259.
- [3] K. Kono, *Drug Delivery Syst.* 17 (6) (2002) 462–470.
- [4] K.S. Soppimath, A.R. Kulkarni, W.E. Rudzinski, T.M. Aminabhavi, *Drug Metab. Rev.* 33 (2) (2001) 149–160.
- [5] R. Langer, M. Karel, *Polym. News* 7 (6) (1981) 250–258.
- [6] R.W. Baker, *Controlled Release of Biologically Active Agents*, Wiley, New York, 1986, pp. 46–50.
- [7] P. Payra, P.K. Dutta, in: S.M. Auerbach, K.A. Carrado, P.K. Dutta (Eds.), *Handbook of Zeolite Science and Technology*, Dekker, New York, 2004, pp. 1–19.
- [8] J.S.N.d. Pino, I.J.A. Padron, M.M.G. Martin, J.E.G. Hernandez, *J. Control. Release* 34 (1995) 25–29.
- [9] W.G. Pond, F.A. Mumpton, *Zeo-Agriculture: Use of Natural Zeolites in Agriculture and Aquaculture*, Westview Press, Boulder, Colo., 1984, pp. 3–31.
- [10] A. Dyer, S. Morgan, P. Wells, C. Williams, *J. Helminthol.* 74 (2000) 137–141.
- [11] K.A. Fisher, K.D. Huddersman, M.J. Taylor, *Chem. Eur. J.* 9 (2003) 5873–5878.
- [12] M. Vallet-Regi, A. Ramila, R.P.D. Real, J. Pe'rez-Pariente, *Chem. Mater.* 13 (2001) 308–311.
- [13] N.K. Mal, M. Fujiwara, Y. Tanaka, T. Taguchi, M. Matsukata, *Chem. Mater.* 15 (2003) 3385–3394.
- [14] N.K. Mal, M. Fujiwara, Y. Tanaka, *Nature* 421 (2003) 350–353.
- [15] B. Munoz, A. Ramila, J. Perez-Pariente, I. Diza, M. Vallet-Regi, *Chem. Mater.* (15) (2003) 500–503.
- [16] D.R. Radu, C.-Y. Lai, J.W. Wiench, M. Pruski, V.S.-Y. Lin, *J. Am. Chem. Soc.* 126 (2004) 1640–1641.
- [17] E.F. Vansant, *Pore Size Engineering in Zeolites*, J. Wiley & Sons, New York, Chichester, 1990.
- [18] T. Kawai, K. Tsutsumi, *Colloid Polym. Sci.* 276 (1998) 992–998.
- [19] N.R.E.N. Impens, P.V.D. Voort, E.F. Vansant, *Micropor. Mesopor. Mater.* 28 (1999) 217–232.
- [20] R. Anwender, I. Nagl, M. Widenmeyer, *J. Phys. Chem. B* 104 (2000) 3532–3544.
- [21] L.A. Summers, *The Bipyridinium Herbicides*, Academic Press, New York, 1980.
- [22] A. Walcarius, L. Lamberts, E.G. Derouane, *Electrochim. Acta* 38 (1993) 2267–2276.
- [23] T. Watanabe, K. Honda, *J. Phys. Chem.* 86 (1982) 2617–2619.
- [24] G. Metz, X. Wu, S.O. Smith, *J. Magn. Reson.* 110 (1994) 219–227.
- [25] P.A. Jacobs, W.I. Mortier, *Zeolite 2* (1982) 226–230.
- [26] X.S. Zhao, G.Q. Lu, *J. Phys. Chem. B* 102 (1998) 1556–1561.
- [27] I.F.J. Vankelecom, S.V. den Broeck, E. Merck, H. Geerts, P. Grobet, J.B. Uytterhoeven, *J. Phys. Chem.* 100 (1996) 3753–3758.
- [28] E. Wiberg, E. Amberger, *Hydrides of the Elements of Main Groups I–IV*, Elsevier Pub. Co., Amsterdam, New York, 1971, pp. 528–530.
- [29] B.R. Shaw, K.E. Creazy, C.J. Lanczyzki, J.A. Sargeant, M. Tirhado, *J. Electrochem. Soc.* 135 (1988) 869–876.
- [30] H.S. Sherry, in: S.M. Auerbach, Kathleen A. Carrado, P.K. Dutta (Eds.), *Handbook of Zeolite Science and Technology*, Dekker, New York, 2004, pp. 1007–1062.
- [31] D. Reichenberg, *J. Am. Chem. Soc.* 75 (1953) 589–597.
- [32] G.E. Boyd, A.W. Adamson, L.S. Myers, *J. Am. Soc. Chem.* 69 (1947) 2836–2848.

- [33] Y.I. Kim, T.E. Mallouk, *J. Phys. Chem.* 96 (1992) 2879–2885.
- [34] S. Motycka, J.G. Nairn, *J. Pharm. Sci.* 68 (1979) 211–215.
- [35] F. Atyabi, H.L. Sharma, H.A.H. Mohammad, J.T. Fell, *J. Control. Release* 42 (1996) 25–28.
- [36] H. Ichikawa, K. Fujioka, M.C. Adeyeye, Y. Fukumori, *Int. J. Pharm.* 216 (2001) 67–76.
- [37] C. Chretien, V. Boudy, P. Allain, J.C. Chaumeil, *J. Control. Release* 96 (2004) 369–378.